

NANO EXPRESS

Open Access



Carrier Transport Properties of MoS₂ Asymmetric Gas Sensor Under Charge Transfer-Based Barrier Modulation

Sun Jun Kim^{1†}, Jae Young Park^{1†}, SangHyuk Yoo^{1†}, Palanivel Umadevi², Hyunpyo Lee¹, Jinsoo Cho^{2*}, Keonwook Kang^{1*} and Seong Chan Jun^{1*}

Abstract

Over the past few years, two-dimensional materials have gained immense attention for next-generation electric sensing devices because of their unique properties. Here, we report the carrier transport properties of MoS₂ Schottky diodes under ambient as well as gas exposure conditions. MoS₂ field-effect transistors (FETs) were fabricated using Pt and Al electrodes. The work function of Pt is higher than that of MoS₂, while that of Al is lower than that of MoS₂. The MoS₂ device with Al contacts showed much higher current than that with Pt contacts because of its lower Schottky barrier height (SBH). The electrical characteristics and gas responses of the MoS₂ Schottky diodes with Al and Pt contacts were measured electrically and were simulated by density functional theory calculations. The theoretically calculated SBH of the diode (under gas absorption) showed that NO_x molecules had strong interaction with the diode and induced a negative charge transfer. However, an opposite trend was observed in the case of NH₃ molecules. We also investigated the effect of metal contacts on the gas sensing performance of MoS₂ FETs both experimentally and theoretically.

Keywords: MoS₂, Field-effect transistor, Schottky diode, Gas sensor, Contact effect, Schottky barrier

Background

In recent years, after the discovery of graphene, two-dimensional (2D) nanomaterials, which have vertically stacked layers connected by van der Waals (vdW) forces, have gained immense attention because of their unique properties [1–5]. Graphene, which is a layered hexagonal structure of carbon, with its unique properties such as high carrier mobility [6, 7], mechanical strength [8], and flexibility [9, 10], has opened up new avenues for nanoelectronic devices. Recently, transition metal dichalcogenides (TMDs), such as MoS₂ and WSe₂, have also been studied because of their higher band gaps as compared to that of graphene [11–15]. Monolayer MoS₂, with a thickness of 6.5 Å is the most widely known 2D-layered TMD. It shows a high mobility of up to ~ 200 cm² V⁻¹ s⁻¹

[16] and on/off ratios exceeding ~ 10⁸ [17]. Furthermore, MoS₂ is a semiconductor with an indirect band gap of 1.2 eV [18] in bulk and a direct band gap of 1.8 eV [19] in a single layer unlike graphene which has zero band gap. This zero band gap of graphene limits its application in nanoelectronic devices.

In order to develop MoS₂ transistors with performance comparable to that of silicon-based devices, many limitations such as the quality of lattice state, fabrication, and contact resistance between the contact metal and MoS₂ have to be overcome. Many of the previous studies in this context have focused on improving the electrical interaction at the interface of MoS₂ and the metal electrodes. This is because contact-related properties include the potential difference, annealing conditions, and area. However, most of these studies assumed symmetric junctions and did not involve both experimental and theoretical analyses. In addition, it is difficult to analyze the carrier behavior of MoS₂ under gas exposure conditions by only observing its band structure modulation. There is limitation for applying this simulation results because this basic band structure cannot provide any specific value for determining

* Correspondence: jscho@gachon.ac.kr; kwkang75@yonsei.ac.kr; scj@yonsei.ac.kr

[†]Sun Jun Kim, Jae Young Park and Sang Hyuk Yoo contributed equally to this work.

²Department of Computer Engineering, Gachon University, Gyeonggi-do 461-701, Republic of Korea

¹Department of Mechanical Engineering, Yonsei University, Seoul 120-749, Republic of Korea

the modulation. Furthermore, although Schottky barrier height (SBH) is believed to be an important factor for determining the electrical response of MoS₂ transistor under gas absorption, the previous studies did not analyze the effect of SBH both theoretically and experimentally.

In this study, we fabricated MoS₂ FETs with asymmetric electrodes, Al and Pt, to observe carrier transport through the Schottky barrier under gas exposure conditions. First, the work function difference in the devices was geometrically mapped by measuring their surface potentials using Kelvin probe force microscopy (KPFM). To design the MoS₂ Schottky diode, the contact effect of the MoS₂/metal interface was analyzed under ambient conditions both theoretically (density functional theory (DFT) calculations) and experimentally (electrical measurements of the symmetric and asymmetric MoS₂ FETs). The electrical response of the diode was measured under gas exposure conditions. This electrical response was then compared with the theoretically calculated SBH change values which makes possible to understand the modulation numerically. The findings of this study provide an insight into the interaction of gas molecules and the MoS₂/metal contact interface in MoS₂-based gas sensing devices.

Method

Fabrication of MoS₂ Devices

We fabricated the MoS₂ Schottky devices using a facile mechanical transfer method. Few-layered flakes of MoS₂ were exfoliated from its bulk crystal, which was purchased from SPI supplies. Using polydimethylsiloxane (PDMS) (“Sylgard 184”, Dow corning), MoS₂ was transferred to highly doped Si/SiO₂ substrates. Pt and Al electrodes (100 nm thick) were deposited on the sample films and were patterned by electron beam lithography using a field emission scanning electron microscope (FE-SEM) (JSM-7001F, JEOL Ltd.). The performance of the MoS₂ devices was evaluated by measuring their source/drain and source/gate voltage modulations (Keithley 2400 source meter) at room temperature.

Surface Potential Measurement

The surface potential of the devices was measured by the interleave mode of electric force microscopy (Nanoscope IV, Veeco) using a PtIr-coated silicon probe tip (SCM-PIT, Veeco) at ambient air condition of 25 °C and 1 bar. The first scan of the tip examined the surface topology of the devices. A subsequent second scan was carried out to measure the electrostatic force between the device surface and the tip.

DFT Calculations

A $\sqrt{3} \times \sqrt{3}$ supercell of MoS₂ was prepared with three Mo atoms and six S atoms (Fig. 3a). A vacuum spacing

of 15 Å was defined in order to prevent the interaction of the images. The lattice constant was calculated to be 3.184 Å, which is in good agreement with the experimental value (3.160 Å). Substrates with six layers of Al or Pt metal atoms (with (111) free surface) were fabricated to construct the interface between the metals and monolayer MoS₂. The lattice constants of Al and Pt substrates were computed to be 4.070 and 3.973 Å, respectively. After the geometry optimization of each structure, monolayer MoS₂ was deposited on the substrate and the configuration was optimized again. A lattice mismatch between MoS₂ and the metal substrates was observed because the monolayer of MoS₂ stretched during the geometry optimizations. The structure of monolayer MoS₂ with gas molecules (including NO₂ and NH₃) was also constructed and optimized using a $\sqrt{3} \times \sqrt{3}$ supercell.

DFT calculations were performed by using VASP (Vienna ab initio simulation package) [20–23]. GGA (generalized gradient approximation)–PBE (Perdew–Burke–Ernzerhof) to exchange-correction functional of PAW (Projector Augmented-wave) method was used with vdW corrections [24–27]. The cutoff energy for the basis set was extended to 500 eV for all the calculations. For the self-consistency and band structure calculations, the electronic energy convergence and atomic force criteria were set to 10^{−5} eV and 0.02 eV/Å, respectively. The K-points for Brillouin-zone sampling were $8 \times 8 \times 1$ (with Gamma (Γ) point centered). For measuring the vdW interactions between the gas molecules and MoS₂, the DFT-D2 method of Grimme was used [28].

Result and Discussion

We prepared MoS₂ devices with two types of electrodes (Al and Pt) and characterized their morphology and thickness using atomic force microscopy (AFM) (Fig. 1a). Figure 1b shows the height of the MoS₂ layer along the cross-section line (shown by the red line in Fig. 1a). The thickness of the MoS₂ sample was 4 nm. To demonstrate the work function difference in the MoS₂ devices with symmetric and asymmetric electrodes, we employed KPFM to measure the contact potential difference between MoS₂ and the probe tip. When the probe tip and sample were close enough, an electrostatic force was applied because of the work function difference between them. The relation between the electrostatic force and work function of the two materials is as follows:

$$F_{\text{electrostatic}} = \frac{q_s q_t}{4\pi\epsilon_0 z^2} + \frac{1}{2} \frac{dC}{dz} (V_{\text{applied}} - V_{\text{contact}})^2$$

where dC/dz is the derivative capacitance between the sample and the tip, q_s is the surface charge, and q_t is the charge of the tip. V_{contact} can be characterized by

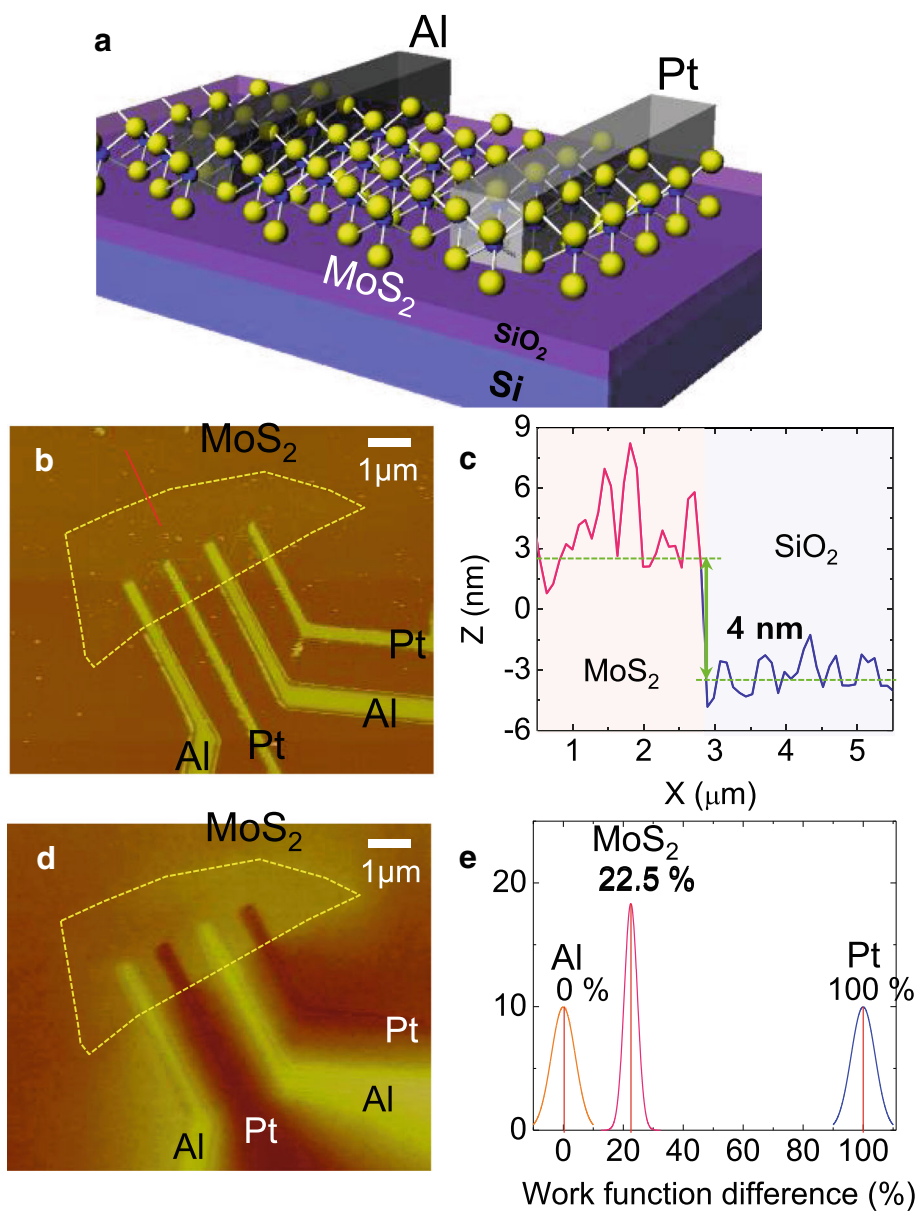


Fig. 1 **a** Schematic diagram of the MoS₂ Schottky diodes with Al and Pt contacts. **b** AFM image of the MoS₂ Schottky diode device with asymmetric metal electrodes (Al/Pt). **c** Cross-sectional analysis of the device for measuring the thickness of MoS₂ layer. **d** Surface potential image of the same device. **e** Normalized distribution of the relative surface potentials of MoS₂, Al, and Pt

the surface potential value [29]. Using the surface potential value, we calculated the work function as

$$V_{\text{contact}} = \Phi_m - \chi_s - \Delta E_{fn} - \Delta\Phi$$

where Φ_m is the work function of the probe tip, χ_s is the electron affinity, ΔE_{fn} is the Fermi-level position from the lowest level of the conduction band, and $\Delta\Phi$ is the modified band bending.

The surface potential mapping of the devices is shown in Fig. 1c. We added the work function value (4.85 eV)

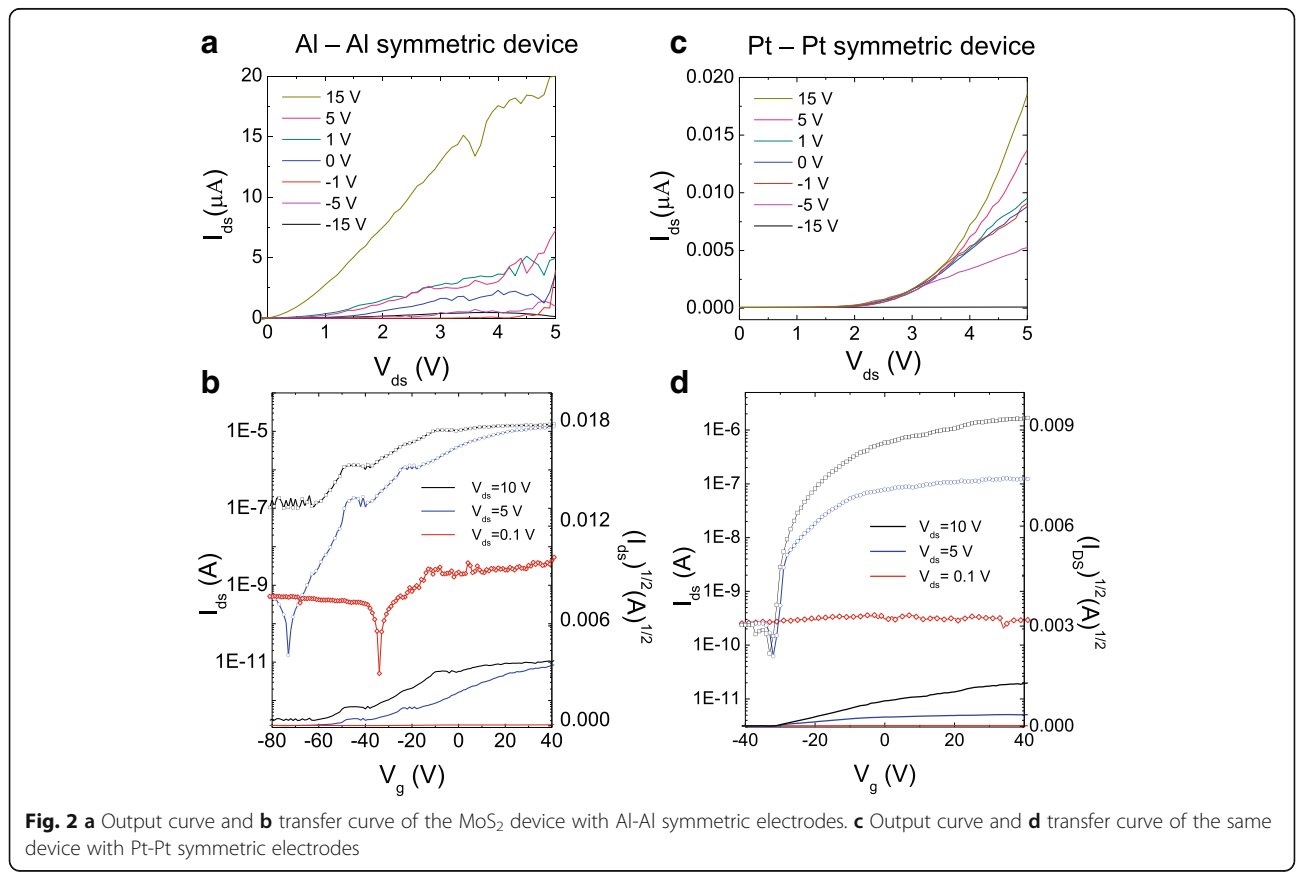
of PtIr-coated Si tip to get the work function of electrode and channel part [30]. Then, normalization process was followed by positioning the percentage value of MoS₂ between Pt and Al as shown in Fig. 1d. The difference between the surface potentials of Al and MoS₂ was 22.5%, which is smaller than that between the surface potentials of Pt and MoS₂ (100%). Unlike Pt, Al has a work function comparable to that of MoS₂. This is because the surface potential of Al is comparable to that of MoS₂. Since, MoS₂ and Al have similar work functions, they can form Ohmic contacts. MoS₂ and Pt exhibit Schottky

contacts because of their large surface potentials. Further studies should be followed to confirm whether the potential modulation occurs under gas absorption for understanding gas sensing mechanism.

To compare the asymmetric junction characteristics of the devices, the current–voltage characteristics of the devices with Al and Pt contacts over the gate voltage range of -15 – 15 V are shown in Fig. 2a, c, respectively. The MoS₂ device with Al contact showed a linear drain current which was much higher than that of the device with Pt contact. The current of the Al contact was more than 1000 times higher than that of the Pt contact. This suggests that the SBH of devices with low-work function metal contacts is low. To further investigate the effect of metal contacts on the MoS₂/metal interface of the devices, their transfer characteristics at different forward bias voltages (0.1, 5, and 10 V) were measured (Fig. 2b, d). In both the cases (Al and Pt contacts), the transfer curves of MoS₂ showed the characteristics of n-type semiconductors, i.e., the current level at positive gate voltages was higher than that at negative gate voltages [31]. At the source–drain bias of 0.1 V, only the device with Al contact showed the on-off tendency. When the bias was increased to 5 V, the on-off ratios of the Al and Pt contacts were approximately 10⁶ and 10³, respectively. As the bias voltage approached

10 V, the off function of the device with Al contact became disabled, while the on-off ratio of the Pt contact increased. This suggests that in order to achieve gas sensing devices with the desired performance over a specific current range, it is imperative to use appropriate metal contacts. In order to determine the threshold voltage of the devices, the $\sqrt{I_{DS}}$ versus gate voltage curve was added to their transfer curves (Fig. 2b, d). This is because it is easier to measure the threshold voltage by smoothing the fluctuations of the $\sqrt{I_{DS}}-V_g$ line. The threshold voltage induced by the $\sqrt{I_{DS}}-V_g$ line for the device with Al electrode was about -70 V, while that for the device with Pt electrode was about -30 V (Fig. 2a, c). The threshold voltage of the device with Al contact was much lower than that of the device with Pt contact. This can be attributed to the lower Schottky height of the Al/MoS₂ interface as compared to that of the Pt/MoS₂ interface. In addition, the threshold voltage of the device with Al contact was strongly modulated by the source–drain voltage. On the other hand, no significant change was observed in the threshold voltage of the device with Pt contact with the drain–source voltage.

To theoretically analyze the electrical states at the metal/MoS₂ interface, DFT calculations were carried out using a MoS₂-on-Al configuration (Fig. 3a, b). Table 1 lists the lattice mismatches and distance h between MoS₂ and the



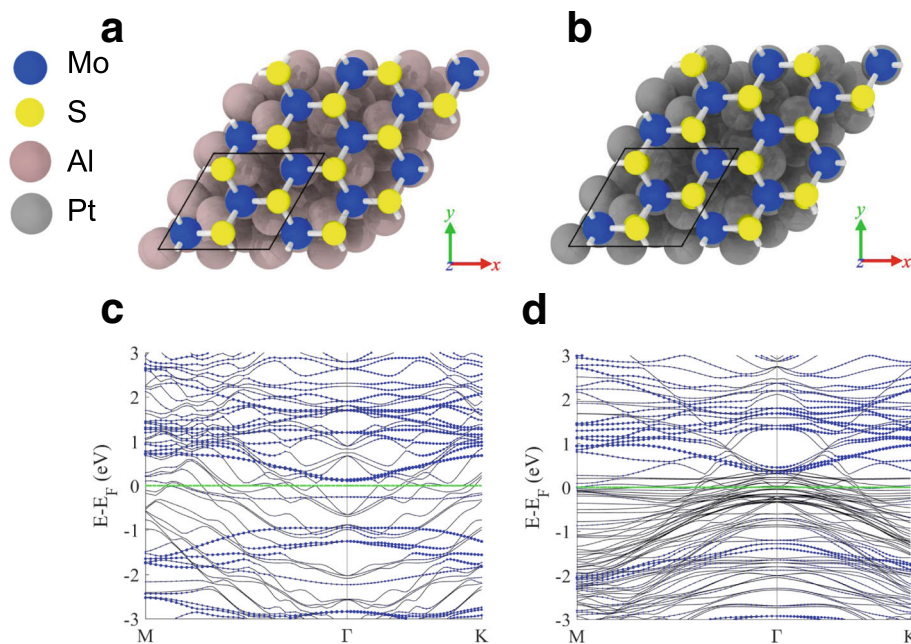


Fig. 3 **a, b** The 3D models of MoS₂ on Al and Pt substrates, which were used in DFT calculations. **c, d** The band structures of these models. Green lines indicate the Fermi energy set by taking zero as the work function of the vacuum level. Blue dashes correspond to the energy bands of monolayer MoS₂. Difference between the value of green lines and the minimum value of blue dashes on the conduction band site is SBH [38]

metal substrates. The values obtained in this study were consistent with those reported previously [32]. The band structures of MoS₂ with the Al and Pt substrates are shown in Fig. 3c, d, respectively. Work function and SBH values are summarized in Table 1. Work function and SBH values are summarized in Table 1. Work function of MoS₂ with Pt substrate (5.755 eV) is well-matched previous results (5.265 eV) [32]. The value of SBH for the device with Al substrate was 72% lower than that for the device with Pt substrate. The reason of SBH difference results from work function difference between Al and Pt; work function of Al is 64% lower than that of Pt. [33] Thus, Al/Pt asymmetric contact systems can function as diodes.

To further examine the performance of Al/Pt asymmetric systems, we fabricated Al/Pt asymmetric metal electrodes

on MoS₂ Schottky devices. Figure 4a shows the current–voltage characteristics of the MoS₂ devices with Al–Al, Pt–Pt, Al–Pt, and Pt–Al contacts (as the order of source and drain). Unlike the symmetric curve of the Al–Al and Pt–Pt devices, the asymmetric diode showed rectifying characteristics in the direction of the MoS₂/Al contact. To investigate the effect of charge transfer on the performance of the devices, we observed their drain currents as a function of the gate bias (Fig. 4b). The transfer curves corresponding to the source–drain voltage were also obtained (Fig. 4c). Figure 4c shows that the threshold voltage shifted from 40 to –40 V with an increase in the source–drain voltage. A similar trend was observed in the case of the symmetrically Al-contacted device. This implies that the Al/MoS₂ contact side affected the carrier transport of the device more than the Pt/MoS₂ contact side.

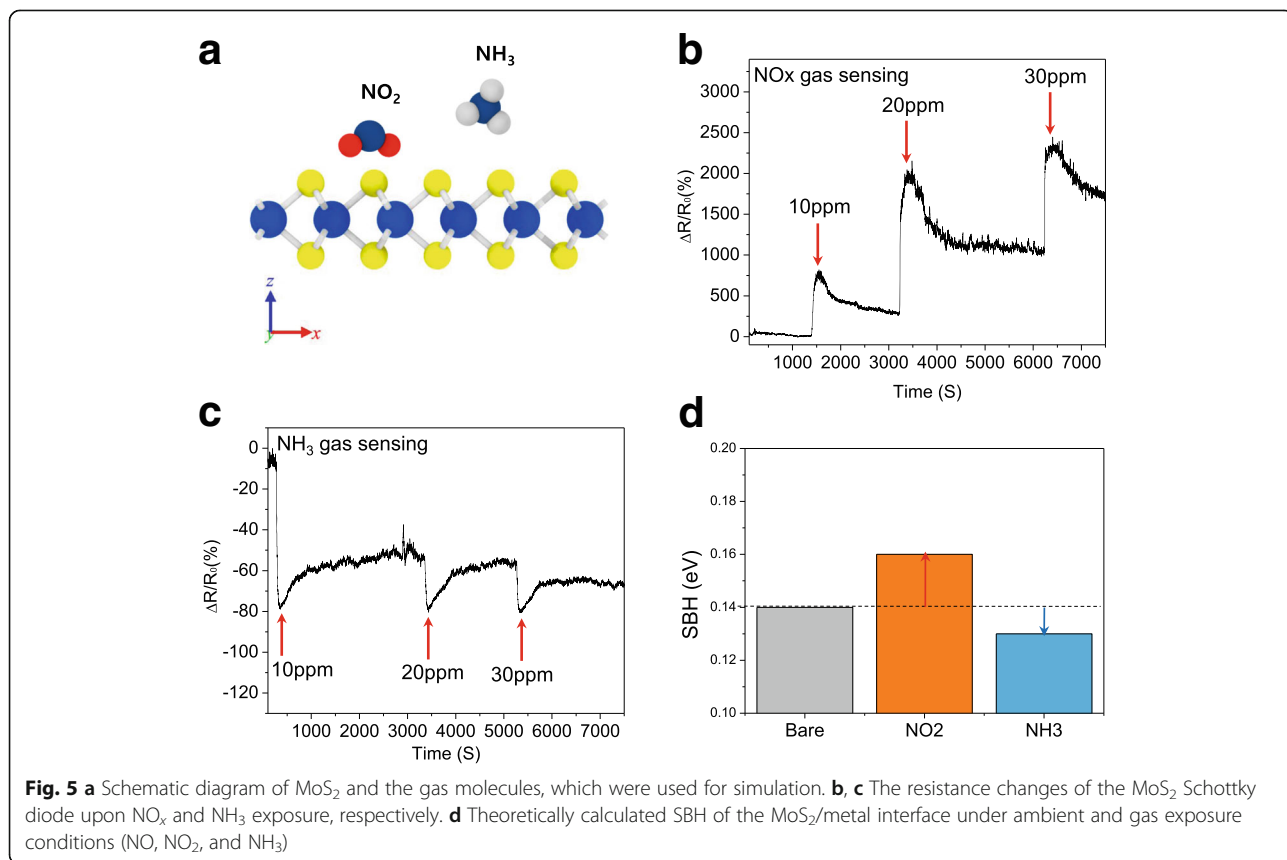
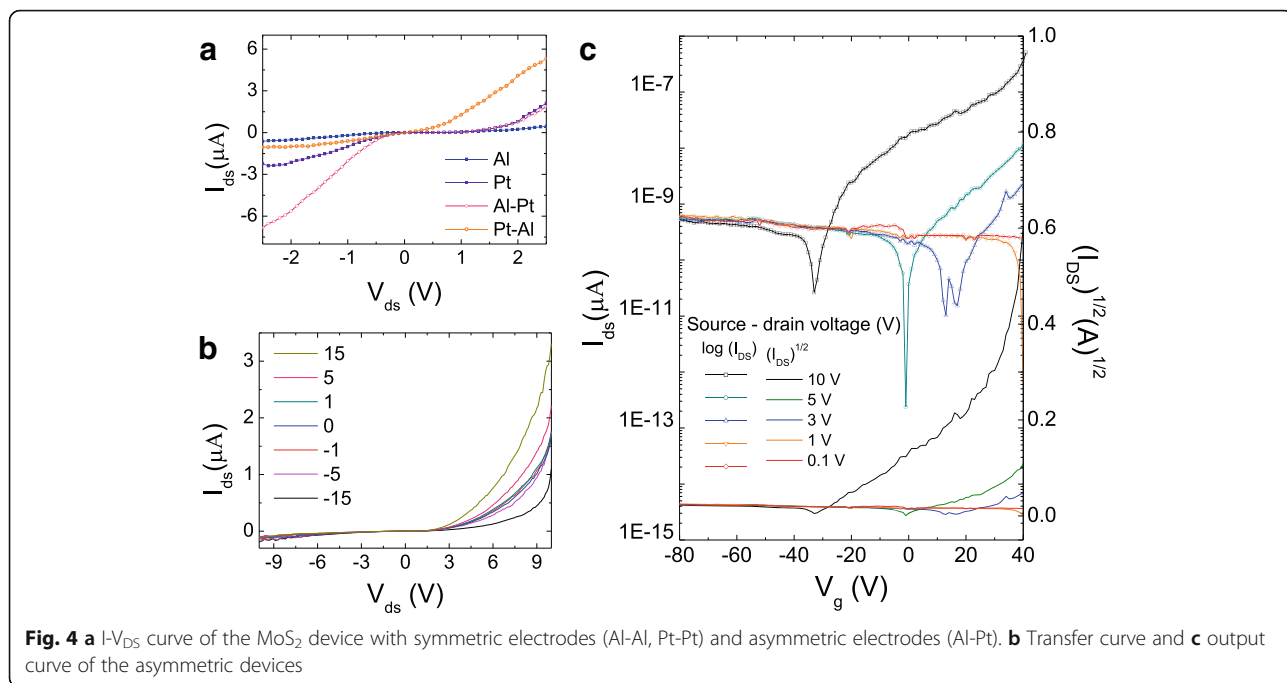
The real-time gas response of the MoS₂ Schottky diode was measured to observe its Schottky barrier modulation with charge transfer. The gas sensitivity of the diode was calculated using the following equation:

$$\frac{\Delta R}{R_{\text{air}}} = \frac{R_{\text{gas}} - R_{\text{air}}}{R_{\text{air}}}$$

where R_{air} and R_{gas} represent the resistance of the MoS₂ Schottky diode under ambient and gas exposure conditions, respectively. Figure 5 shows the gas sensing ability (change in resistance with time) of the MoS₂ Schottky device for NO_x and NH₃ molecules (10, 20, and 30 ppm)

Table 1 Lattice mismatch was calculated using the lattice constant of MoS₂ ($a = 5.514 \text{ \AA}$). Distance h is the difference between the averaged z -position values of S and Al at the interface. Work function was computed by the equation, $W = E_{\text{fermi}} - \phi_{\text{vac}}$, E_{fermi} is the Fermi energy of the total system (MoS₂ + metal substrate), and ϕ_{vac} is the vacuum potential of the system. SBH was calculated as mentioned in the legend of Fig. 3

	Metal substrate	Al (111)	Pt (111)
Structural parameters	Lattice mismatch (%)	4.38	1.39
	Distance h (Å)	2.517	2.218
Electronic parameters	Work function (eV)	4.680	5.265
	SBH (eV)	0.1423	0.506



at an applied source-drain bias of 3 V. Since NO_x is a strong electron acceptor, and hence is a p-doping material, the resistance of the device increased with an increase in the gas exposure because of the negative charge injection at the interface of MoS_2 [34]. The p-doping of MoS_2 increased its Schottky barrier, which in turn increased the contact resistance at the MoS_2 /metal interfaces. The gas absorption dependence of the signal response was also observed. The sensitivity of the device increased with an increase in the gas concentration, indicating an increase in its charge transfer. The resistance of the device on the other hand decreased upon exposure to NH_3 (Fig. 5c). This is because NH_3 donates electrons to MoS_2 , thus decreasing its Schottky barrier [35]. The measured gas sensitivity of NH_3 was much lower than that of NO_x , indicating that charge transfer in the presence of NH_3 was lower than that in the presence of NO_x [36]. In addition, a slight dependence of gas concentration was also observed after the current fluctuation in each step. With an increase in the NH_3 concentration, the resistance of the device decreased. This is because the MoS_2 /Al interface showed lower SBH values at higher NH_3 concentrations. To confirm these results theoretically, we calculated the SBH of the MoS_2 /Al interface, which was in contact with various kinds of gas molecules (Fig. 5d). Kang et al. previously discussed about Schottky barrier theory of MoS_2 /metal contact and explained the carrier transport through contact side by using three types of model [37]. According to band diagram illustrated in this paper, Schottky barrier modulation occurs at the boundary of electrode and channel. So, we designed the composite structure which has uniformly distributed Schottky barrier to facilitate the observation of Schottky barrier modulation according to gas absorption. However, the model is not applied to all situations. Type 3 showed that Schottky barrier was not formed at the directly contacted interface of MoS_2 and metal because of the strong metallization effect. The metals which have strong adhesion with MoS_2 like Ti and Mo are classified as Type 3. To explore various contact effects in the metal/ MoS_2 composite, careful consideration should be followed to design the model structure (Additional file 1: Figure S1 and S2). Only the Al side was selected for calculating the barrier height because the barrier with Pt electrode did not disturb the carrier transport under the forward bias. NO_2 and NH_3 were selected for the modulation of the Schottky barrier of the MoS_2 /Al interface. This Schottky barrier was compared with that observed in pristine condition (Table 1). The theoretically calculated barrier heights for NO_2 and NH_3 were 0.16 and 0.13 eV, respectively. This result shows that NO_2 and NH_3 induced charge transfer in different directions. The Schottky barrier was affected more by NO_2 than by NH_3 . These results were consistent with the experimental results. The results also demonstrate that MoS_2

Schottky diodes have great potential to be used in next-generation gas sensing devices.

Conclusion

In this study, we investigated the effect of the contact material on the properties of MoS_2 asymmetric FETs under ambient and gas exposure conditions. The KPFM results showed that Pt had the highest work function followed by MoS_2 and Al. The DFT results predicted that the SBH of the MoS_2 /metal interface was higher for the metal with higher work function. This is consistent with the experimental results obtained for the symmetric (Al-Al and Pt-Pt) and asymmetric (Al-Pt) FETs fabricated in this study. The absorption of NO_x resulted in a strong gas response and in an increase in the resistivity of the device. Opposite trends were observed in the case of NH_3 . These results were consistent with the theoretically calculated SBH values. This study emphasizes on the importance of choosing appropriate metal contacts for developing MoS_2 gas sensors with desired performance.

Additional file

Additional file 1: Figure S1. Configurations of adsorption molecules on the MoS_2 with Al substrate. **Figure S2.** Band structure calculation of pristine MoS_2 with gas adsorption. (DOCX 310 kb)

Abbreviations

AFM: Atomic force microscopy; DFT: Density functional theory; FET: Field-effect transistor; KPFM: Kelvin probe force microscopy; SBH: Schottky barrier height; TMDs: Transition metal dichalcogenides; V_{ds} : Source-drain voltage; vdW: van der Waals

Acknowledgements

This research was supported by Nano-Material Technology Development Program (NRF-2017M3A7B4041987) through the National Research Foundation of Korea (NRF) funded by the Ministry of Science, ICT and Future Planning, by the Korea Ministry of Environment as "Global Top Project (2016002130005)", and the Development of diagnostic system for mild cognitive impairment due to Alzheimer's disease (2015-11-1684).

Authors' Contributions

SJK and JYP conducted the experiment and wrote this manuscript. SHY supported and verified the results by theoretical method. UP verified the simulation data. HL supported the experiment. JC, KK, and SCJ are the supervisors. All authors read and approved the final manuscript.

Competing Interests

The authors declare that they have no competing interests.

Publisher's Note

Springer Nature remains neutral with regard to jurisdictional claims in published maps and institutional affiliations.

Received: 23 March 2018 Accepted: 2 August 2018

Published online: 04 September 2018

References

1. Novoselov K, Geim A (2007) The rise of graphene. *Nat Mater* 6:183–191
2. Schedin F, Geim A, Morozov S, Hill E, Blake P, Katsnelson M, Novoselov K (2007) Detection of individual gas molecules adsorbed on graphene. *Nat Mater* 6:652–655

3. Mehrali M, Sadeghinezhad E, Latibari ST, Kazi SN, Mehrali M, Zubir MNBM, Metselaar HSC (2014) Investigation of thermal conductivity and rheological properties of nanofluids containing graphene nanoplatelets. *Nanoscale Res Lett* 9:15
4. Romasanta LJ, Hernández M, López-Manchado MA, Verdejo R (2011) Functionalised graphene sheets as effective high dielectric constant fillers. *Nanoscale Res Lett* 6:508
5. Fan X-L, An Y-R, Guo W-J (2016) Ferromagnetism in transitional metal-doped MoS₂ monolayer. *Nanoscale Res Lett* 11:154
6. Schwierz F (2010) Graphene transistors. *Nat Nanotech* 5:487–496
7. Du X, Skachko I, Barker A, Andrei EY (2008) Approaching ballistic transport in suspended graphene. *Nat Nanotech* 3:491–495
8. Havener RW, Ju S-Y, Brown L, Wang Z, Wojcik M, Ruiz-Vargas CS, Park J (2011) High-throughput graphene imaging on arbitrary substrates with widefield Raman spectroscopy. *ACS Nano* 6:373–380
9. Stöberl U, Wurstbauer U, Wegscheider W, Weiss D, Eroms J (2008) Morphology and flexibility of graphene and few-layer graphene on various substrates. *Appl Phys Lett* 93:051906
10. Wei N, Xu L, Wang H-Q, Zheng J-C (2011) Strain engineering of thermal conductivity in graphene sheets and nanoribbons: a demonstration of magic flexibility. *Nanotech* 22:105705
11. Radisavljevic B, Radenovic A, Brivio J, Giacometti V, Kis A (2011) Single-layer MoS₂ transistors. *Nat Nanotech* 6:147–150
12. Radisavljevic B, Whitwick MB, Kis A (2011) Integrated circuits and logic operations based on single-layer MoS₂. *ACS Nano* 5:9934–9938
13. Liu H, Neal AT, Ye PD (2012) Channel length scaling of MoS₂ MOSFETs. *ACS Nano* 6:8563–8569
14. Hao L, Liu Y, Du Y, Chen Z, Han Z, Xu Z, Zhu J (2017) Highly enhanced H₂ sensing performance of few-layer MoS₂/SiO₂/Si heterojunctions by surface decoration of Pd nanoparticles. *Nanoscale Res Lett* 12:567
15. Lu S-C, Leburton J-P (2014) Electronic structures of defects and magnetic impurities in MoS₂ monolayers. *Nanoscale Res Lett* 9:676
16. Novoselov K, Jiang D, Schedin F, Booth T, Khotkevich V, Morozov S, Geim A (2005) Two-dimensional atomic crystals. *Proc Natl Acad Sci U S A* 102: 10451–10453
17. Wu W, De D, Chang S-C, Wang Y, Peng H, Bao J, Pei S-S (2013) High mobility and high on/off ratio field-effect transistors based on chemical vapor deposited single-crystal MoS₂ grains. *Appl Phys Lett* 102:142106
18. Kam K, Parkinson B (1982) Detailed photocurrent spectroscopy of the semiconducting group VIB transition metal dichalcogenides. *J Phys Chem* 86:463–467
19. Mak KF, Lee C, Hone J, Shan J, Heinz TF (2010) Atomically thin MoS₂: a new direct-gap semiconductor. *Phys Rev Lett* 105:136805
20. Kresse G, Hafner J (1993) Ab initio molecular dynamics for liquid metals. *Phys. Rev B* 47:58–561
21. Kresse G, Hafner J (1994) Ab initio molecular-dynamics simulation of the liquid-metal amorphous-semiconductor transition in germanium. *Phys. Rev B* 49:14251–14269
22. Kresse G, Furthmüller J (1996) Efficiency of ab-initio total energy calculations for metals and semiconductors using a plane-wave basis set. *Comp. Mater Sci* 6:15–50
23. Kresse G, Furthmüller J (1996) Efficient iterative schemes for Ab initio total-energy calculations using a plane-wave basis set. *Phys. Rev B* 54:11169–11186
24. Blöchl PE (1994) Projector augmented-wave method. *Phys. Rev B* 50:17953–17979
25. Kresse G, Joubert D (1999) From ultrasoft pseudopotentials to the projector augmented-wave method. *Phys. Rev B* 59:1758–1775
26. Perdew JP, Burke K, Ernzerhof M (1996) Generalized gradient approximation made simple. *Phys. Rev Lett* 77:3865–3868. <https://journals.aps.org/prl/abstract/10.1103/PhysRevLett.78.1396>
27. Perdew JP, Burke K, Ernzerhof M Generalized gradient approximation made simple [Phys. Rev. Lett. 77, 3865 (1996)]. *Phys. Rev. Lett* 78:1396–1396
28. Grimme S (2006) Semiempirical GGA-type density functional constructed with a long-range dispersion correction. *J Comput Chem* 27:1787–1799
29. Yoon HS, Joe H-E, Kim SJ, Lee HS, Im S, Min B-K, Jun SC (2015) Layer dependence and gas molecule absorption property in MoS₂ Schottky diode with asymmetric metal contacts. *Sci Rep* 5:10440
30. Lv Y, Cui J, Jiang ZM, Yang X (2012) Nanoscale electrical property studies of individual GeSi quantum rings by conductive scanning probe microscopy. *Nanoscale Res Lett* 7:659
31. Chua L-L, Zaumseil J, Chang J-F, Ou ECW, Ho PKH, Siringhaus H, Friend RH (2005) General observation of n-type field-effect behaviour in organic semiconductors. *Nat* 434:194–199
32. Zhong H, Quhe R, Wang Y, Ni Z, Ye M, Song Z, Pan Y, Yang J, Yang L, Lei M, Shi J, Lu J (2016) Interfacial properties of monolayer and bilayer MoS₂ contacts with metals: beyond the energy band calculations. *Sci Rep* 6:21786
33. Tipler PA, Llewellyn RA (2008) *Modern physics*. Freeman. https://scholar.google.co.kr/scholar?hl=ko&as_sdt=0%2C5&q=Tipler+PA%2C+Llewellyn+RA+%282008%29+Modern+physics.+Freeman&btnG=
34. Tuyen LT, Potje-Kamloth K, Liess H-D (1997) Electrical properties of doped polypyrrole/silicon heterojunction diodes and their response to NO_x gas. *Thin Solid Films* 292:293–298
35. Gao X, Xue Q, Hao L, Zheng Q, Li Q (2007) Ammonia sensitivity of amorphous carbon film/silicon heterojunctions. *Appl Phys Lett* 91:122110
36. Yue Q, Shao Z, Chang S, Li J (2013) Adsorption of gas molecules on monolayer MoS₂ and effect of applied electric field. *Nanoscale. Res. Lett* 8:425
37. Kang J, Liu W, Sarkar D, Jena D, Banerjee K (2014) Computational study of metal contacts to monolayer transition-metal dichalcogenide semiconductors. *Phys Rev X* 4:031005
38. Chen W, Santos EJG, Zhu W, Xaxiras E, Zhang Z (2013) Tuning the electronic and chemical properties of monolayer MoS₂ adsorbed on transition metal substrates. *Nano Lett* 13:509–514

Submit your manuscript to a SpringerOpen[®] journal and benefit from:

- Convenient online submission
- Rigorous peer review
- Open access: articles freely available online
- High visibility within the field
- Retaining the copyright to your article

Submit your next manuscript at ► springeropen.com